Asian Journal of Basic Science & Research
Volume 8, Issue 2, Pages 143-154, April-June 2026

Determination of Kinetics and Thermodynamics Parameters for Congo Red and Methylene Blue Colorants Adsorption with Ground Guava Seed

Denis A. Cabrera-Munguia[1], Jesús A. Martínez-Pérez[1], Sofía A. Hernández-Jasso[1], Lesly Katleya Usme Duque[1], Lucia F. Cano-Salazar[1], Tirso E. Flores Guia[1] & Jesús A. Claudio-Rizo[1*]

[1]Materiales Avanzados, Facultad de Ciencias Químicas, Universidad Autónoma de Coahuila, Saltillo, Coahuila, México.
Corresponding Author (Jesús A. Claudio-Rizo) Email: jclaudio@uadec.edu.mx[*]

DOI: https://doi.org/10.38177/ajbsr.2026.8213

Article Received: 23 April 2026 *Article Accepted: 25 June 2026* *Article Published: 27 June 2026*

ABSTRACT

Guava seeds were dried and ground to be use as adsorbent of model waters with methylene blue (MB) and Congo red (CR) colorants. First, the effect of drying temperature on guava seed was analyzed using Fourier Transform Infrared Spectroscopy (FTIR). Once the appropriate drying temperature is selected, the effect of colorant concentration, temperature, and contact time in the adsorption process mediated by guava seed is studied. The concentrations of dye solutions were 20, 40, 60, 80 y 100 ppm, and were undergone to constant agitation (200 rpm). Samples of colorant were taken by triplicate measure in a UV-Vis spectrometer, this procedure was repeated at 30, 40 and 50ºC. The kinetics analysis indicates a second-rate order, achieving equilibria after 2 or 3 h of contact. In both cases, the data were fitted to a Langmuir isotherm, obtaining a maximum adsorption capacity of 16 mg and 24 mg of colorant per gram of adsorbent for MB and CR, respectively. With this information it was possible to estimate the surface area of ground guava seed obtaining a value of 38.4 to 39.1 m^2/ g. In addition, the thermodynamic analysis indicated that MB adsorption is exothermic (physisorption) and is mediated by its positive charges attracted to hydroxyl and carboxyl groups found in guava seed dried at 80ºC (G80). While CR adsorption is also exothermic (chemisorption) but in this case amine and azo groups are attracted by hydrogen binding with the hydroxyl groups of guava seed.

Keywords: Guava Seed; Methylene Blue; Congo Red; Adsorption; Kinetics; Langmuir Isotherm; Entropy, Enthalpy; Physisorption; Chemisorption..

1.0. Introduction

MB and CR are both soluble dyes applied in the textile industry to color leather and cotton, as well as in the paper manufacturing industry [1]. Other applications of MB include chemical indicators, histology, and aquaculture; however, the high dye discharges from the textile, and paper industries are the main pollution source [2]. Both dyes are synthetic and have complex chemical structures, are persistent, and resist photolysis and biodegradation, causing sunlight blockage in aquatic ecosystems and environmental pollution [3].

Since MB and CR are cationic and anionic dyes, respectively. The appropriate wastewater treatment methods are membrane filtration (nanofiltration, ultrafiltration, and reverse osmosis), coagulation and flocculation, advanced oxidation processes (photocatalysis, ozonation, and Fenton process), and adsorption [4], [5]. This latter stands out for its low cost, simple design, and high efficiency. Adsorption is a surface phenomenon that depends on surface area and solution pH, and its mechanism can be mediated by electrostatic interactions, π-π interactions, van der Waals forces, and hydrogen bonding [6], [7]. The most common materials used in adsorption are clays, zeolites, biopolymers (chitin, chitosan), metal oxides (Fe_3O_4, ZnO, CuO), carbon-based materials, and industrial and agricultural wastes [8], [9].

Nowadays, industrial and agricultural waste has gained attention due to its low or zero cost, the absence of chemical synthesis, and its potential for profitable waste management [10], [11]. In this way, guava seed is a promising option to be applied as a biosorbent for dyes due to its chemical composition of cellulose, hemicellulose, and lignin, which are naturally negatively charged with hydroxyl and carboxyl groups, making it ideal for basic dyes such as

MB. Also, guava seeds can be converted into a carbonaceous material, and its surface can be modified by chemical activation by acids or basic chemical agents [12], [13].

Therefore, this research presents a kinetic and thermodynamic study of the MB and CR adsorption performed by guava seeds (Figure 1). The thermal treatment of guava seeds was necessary to determine the appropriate temperature for preserving the largest number of functional groups that can participate in dye adsorption. Later, the effects of contact time and dye concentration were analyzed to determine the maximum adsorption capacity. This data was useful for calculating an approximate surface area instead of performing N_2 physisorption experiments. Finally, the adsorption temperature was varied to calculate thermodynamic parameters and correlate them with the possible mechanism of adsorption of guava seed.

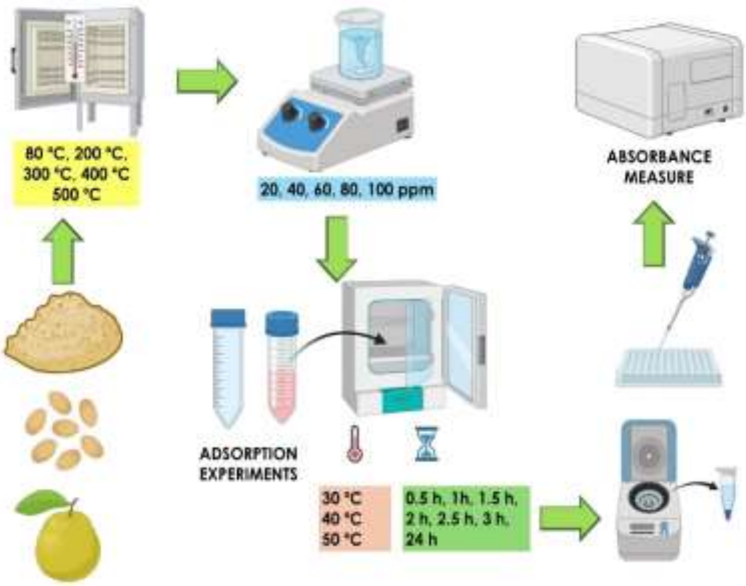

Figure 1. Perspective of ground guava seed as a biosorbent for methylene blue and Congo red adsorption, varying the colorant concentration, time of contact, and adsorption temperature. *Created in BioRender. Cabrera, D. (2026) https://BioRender.com/7cf5vns*

1.1. Study objectives

1) Select the optimal drying temperature for Guava seed to preserve the functional groups that can capture dye molecules.

2) Fit the experimental data with a suitable kinetic model.

3) Calculate the maximum adsorption capacity and the adsorption equilibrium constant with the Langmuir isotherm.

4) Determine the surface area of the guava seed with the maximum adsorption capacity.

5) Estimate the enthalpy and entropy parameters with the van't Hoff and Gibbs-Helmholtz equations.

6) The kinetics and thermodynamics calculations were correlated with the data obtained from FTIR to predict the interaction mechanisms of guava seed with cationic and anionic dyes.

2.0. Literature

It is not new that Guava biomass is used as a biosorbent for organic compounds and heavy metal ions [14], [15], [16]. Indeed, guava biomass, such as the seed, peel, and leaf, has been applied as a biosorbent for dyes like brilliant green, methyl violet 2B, Congo red, methylene blue, and tartrazine. However, as indicated in Table 1, cellulose from guava biomass is typically modified with chemical agents such as phosphoric acid, hydrochloric acid, or zinc chloride or decorated with manganese compounds. All these chemical modifications generally involve the obtaining of carbon activated from guava biomass.

But this research proposes the application and exploitation of the natural chemical functional groups of guava seed, without further chemical modification. The main idea is to select a suitable thermal treatment to preserve as many functional groups as possible for dye adsorption, without the need for any chemical modification. Thus, the importance of this research is to evaluate the use of ground guava seed as a promising adsorbent of CR and MB dyes, and correlate the FTIR characterization with the kinetic and thermodynamic parameters calculated from the fitting of the experimental data, to suggest which are the main functional groups involved in adsorption, and indicate if the adsorption is endothermic or exothermic.

Table 1. Summary of recent studies on raw and chemically modified guava biomass (leaf, bark, and seed) for dye adsorption, including maximum capacities and experimental parameters.

Guava biomass	Chemical modification	Dye	Adsorption capacity	Reference
Guava seeds	Activated carbon-derived guava seed using phosphoric acid	Brilliant green	80.5 mg/g	[12]
Guava peel	Activated carbon-derived guava peel using zinc chloride	Methyl violet 2B	169.9 mg/g	[17]
Guava leaf	Activated carbon-derived guava leaf using phosphoric acid	Congo red	47.64 mg/g	[18]
Guava leaf	Activated carbon-derived guava leaf using hydrochloric acid	Methylene blue	Not mentioned	[19]
Guava leaf	MnO_2 particles growing on cellulose guava leaf	Methylene blue	28 mg/g	[20]
Guava seed	Activated carbon-derived guava seed using zinc chloride	Tartrazine	1.6 mg/g	[21]
Guava leaf	Manganese ferrite ($MnFe_2O_4$) precipitate over guava leaf power by co-precipitation method	Methylene blue	5-21.5 mg/g	[22]

3.0. Methodology

3.1. Guava seed recovery and thermal treatment

First, the guavas were blended with water, and the seeds were separated from the pulp using a sieve. Then, the seeds were washed with water and blended again to eliminate fruit waste. This process was repeated twice. Once the seed was clean, it was dried using a drying oven at 40ºC overnight. Then, seeds were ground using a blender until a fine powder (400 μm) was obtained. The powder was heated up to 80, 200, 300, 400, and 500 °C during 4 h, and labeled as G80, G200, G300, G400, and G500.

3.2. Fourier Transform Infrared Spectroscopy

The functional groups of guava seeds treated at different temperatures were analyzed by infrared spectroscopy using a *Perkin Elmer Frontier* spectrophotometer coupled to an attenuated total reflectance (ATR) accessory. The spectra were acquired over the range 4000 to 600 cm^{-1} with a resolution of 4 cm^{-1}.

3.3. Methylene blue and Congo red adsorption experiments

Stock solutions of MB and CR were prepared at 100 ppm to construct the calibration curve. The calibration curves found for MB (Eq. 1) and CR (Eq. 2), respectively, are:

$$A_{MB} = 0.1357 + 0.0262_{ppm_{MB}} \quad (1)$$

$$A_{CR} = 0.0529 + 0.0168_{ppm_{CR}} \quad (2)$$

Where A_{MB} and ppm_{MB} represent the absorbance and concentration of MB in parts per million, absorbance was measured at 685 nm using a *ThermoScientific MultiSkan Sky* spectrophotometer. Also, A_{CR} and ppm_{CR} are the absorbance measured at 498 nm and the dye concentration in mg per liter of water. In a typical experiment, the kinetic adsorption curves of MB and CR were obtained at 40ºC using a 30 mL dye solution with an initial concentration of 100 ppm and 0.15 g of guava seed, corresponding to 0.5% adsorbent by weight relative to the dye solution. Then, triplicate 200 μL samples were collected every 30 minutes for 4 h, and a final measure was taken at 24 h. The samples were centrifuged in Eppendorf tubes at 4000 rpm, and 100 μL of each supernatant was transferred to a 96-well microplate for absorbance measurement. The experimental data of both dyes were adjusted to find a suitable kinetic model.

The above experiments were repeated using initial concentrations of 20, 40, 60, 80, and 100 ppm while maintaining the same adsorption temperature. Then, the experimental data were fitted to the Langmuir model, and the maximum adsorption capacity (q_m) of each dye was calculated. This value was taken as a reference to calculate the surface area via Langmuir monolayer adsorption. Finally, the concentration variation from 20 to 100 ppm was repeated at 30, 40, and 50ºC to find the Langmuir adsorption constant (K_L) for each temperature. These values were used to calculate the Gibbs free energy, entropy, and enthalpy for MB and CR adsorption

░4.0. Results and Discussions

4.1. ATR-FTIR

The ATR-FTIR spectra of G80, G200, G300, G400, and G500 is shown in Figure 2. In general, all samples showed a broad band around 3350 cm-1, assigned to O-H and N-H stretching vibrations, which practically disappear in G500 samples. The aliphatic C-H stretches at 2930 cm^{-1} and 2860 cm^{-1} disappear in the sample G300. The band at 1745 cm^{-1} is assigned to carbonyl groups (C=O), and the bands at 1240 and 1030 cm-1, which correspond to ester groups, also disappear at 300ºC [23]. These results indicate that guava seeds lose their primary functional groups at

Asian Journal of Basic Science & Research
Volume 8, Issue 2, Pages 143-154, April-June 2026

temperatures above 200ºC. As these bands are more intense at 80ºC, this temperature was selected for adsorption experiments.

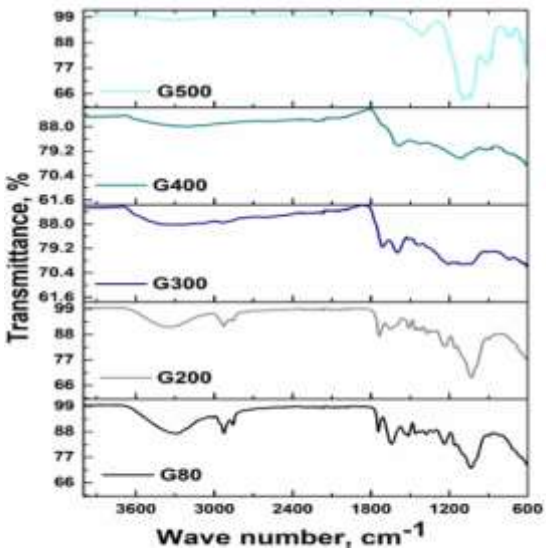

Figure 2. ATR-FTIR spectra of Guava seed heated up to 80, 200, 300, 400, and 500ºC.

4.2. Adsorption kinetics

The kinetic study measures the adsorbate uptake rate by the adsorbent, an important parameter, especially when the adsorption process is to be industrialized. Figure 3(a) shows the adsorption curves of MB and CR as a function of contact time. From this plot, MB adsorption is faster than that of CR; however, both dyes reach the same concentration after 4 h of contact time. Figure 3 (b) indicates that experimental data were fitted to a pseudo-second order, which follows Eq. (3) [24], [25]:

$$\frac{t}{q_t} = \frac{1}{k_2 q_e^2} + \frac{t}{q_e} \qquad (3)$$

Where, t is time in minutes, q_e are the mg of dye adsorbed by a gram of adsorbent in adsorption equilibria, q_t are the mg of colorant adsorbed per gram of adsorbent at any time, and k_2, the kinetics constant of a pseudo-second order.

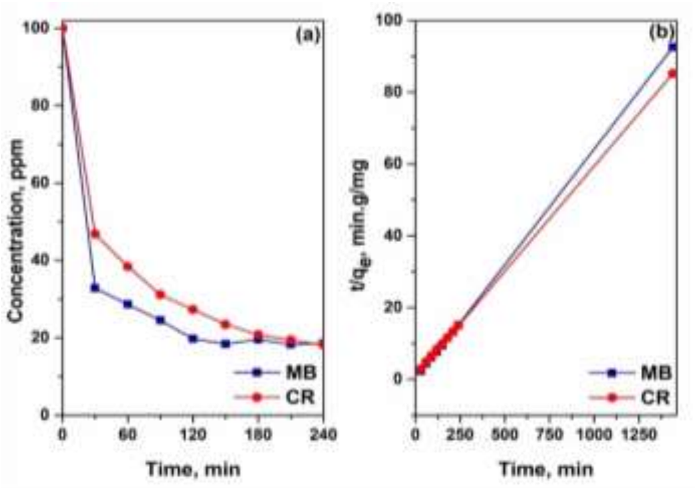

Figure 3. (a) Adsorption curve of MB and CR at 40ºC, and (b) fitting of adsorption data to a pseudo-second order rate, using an initial concentration of 100 ppm of MB and CR.

Asian Journal of Basic Science & Research
Volume 8, Issue 2, Pages 143-154, April-June 2026

Table 2 depicts the kinetics constant values of MB and CR at different initial concentrations at 40ºC. For MB, the kinetic values are practically constant, whereas with CR, the kinetic constant decreases as the dye concentration increases. This is probably due to the larger size of the CR molecule than the MB, as well as the negative charges of the CR that hinder adsorption when its concentration is increased.

Table 2. Second-rate order kinetics constants (k_2), and adsorption capacity at equilibrium conditions (q_e) calculated at 40ºC for MB and CR at different colorant concentrations.

Dyes	**MB**		**CR**	
Initial concentration, ppm	**k_2, g/mg.min**	**q_e, mg MB/g G80**	**k_2, g/mg.min**	**q_e, mg CR/g G80**
20	0.0134	4.50	0.0467	3.41
40	0.0113	7.74	0.0282	7.03
60	0.0056	11.29	0.0080	10.66
80	0.0169	13.64	0.0085	13.62
100	0.0751	15.58	0.0028	17.15

4.3. Langmuir isotherm

The kind of adsorbents whose experimental data follow the Langmuir isotherm are commonly solid and microporous materials or with homogeneous chemical surface (surface active sites). The adsorption is characterized by the formation of a monolayer. The experimental data of different initial concentrations (20, 40, 60, 80, and 100 ppm) at 30, 40, and 50ºC was well-fitted to the Langmuir model, whose mathematical expression is represented in Eq. (4) [24], [25]:

$$\frac{C_e}{q_e} = \frac{1}{q_m K_L} + \frac{C_e}{q_m} \quad (4)$$

Where Ce (mg/L) is the concentration of the adsorbate at the equilibrium, K_L (L/mg) is the Langmuir constant of adsorption. While q_e and q_m (mg/g) are the adsorption capacity at the equilibrium and the maximum adsorption capacity when the monolayer is saturated. Table 2 indicates that as temperature increases, the equilibrium constant (K_L) decreases in both MB and CR, but the effect is more pronounced in CR. These findings suggest an exothermic process for both dyes. Another important observation is that q_m remains constant for MB adsorption, no matter the temperature, while for CR the q_m is increased by 15%.

The equilibria parameter R_L is calculated as [24], [25] with Eq. (5). The value of $R_L>1$ is indicative of an unfavorable isotherm, $R_L=1$ expresses a linear isotherm, values of $0<R_L<1$ indicate a favorable isotherm, while a $R_L=0$ is referred to as an irreversible isotherm (chemisorption).

$$R_L = \frac{1}{1 + K_L C_o} \quad (5)$$

The values of R_L shown in Table 3 are calculated using an initial concentration (C_o) of 100 ppm. The values are close to zero for a chemisorption process, but when an initial concentration of 20 ppm is used, the RL parameter is in the range between zero and one, indicating a favorable isotherm. Thus, guava seed for both colorants is a promising adsorbent when a low initial concentration of dye is applied, which is very common when adsorption is used as a second stage in a tandem wastewater treatment.

Table 3. Estimation of equilibrium constant adsorption (K_L), maximum adsorption capacity (q_m), and the equilibrium parameter (R_L) obtained by the Langmuir isotherm model for MB and CR at 30, 40, and 50 ºC.

Dyes	**MB**			**CR**		
Temperature, ºC	**K_L, L/mg**	**q_m, mg MB/g G80**	**R_L**	**K_L, L/mg**	**q_m, mg CR/g G80**	**R_L**
30	0.3244	15.97	0.0299	0.3471	17.44	0.0280
40	0.2940	15.70	0.0329	0.1466	20.33	0.0639
50	0.2124	15.97	0.0450	0.0653	23.98	0.1328

4.4. Surface area of guava seed

Instead of performing N_2 adsorption isotherms, the surface area of guava seed was calculated using the MB adsorption technique, and Eq. (6) [26]:

$$SSA = \frac{q_m \times N_A \times A_{MB}}{M_{MB}} \quad (6)$$

Where SSA is the specific surface area (m^2/g), q_m (mg/g) is the maximum adsorption capacity. N_A is the Avogadro number (6.022 x10^{23} molecules per mol), A_{MB} is the surface area of MB molecule, taking a value of 130 $Å^2$, and M_{MB} is the molecular weight of MB (319.85 g per mol). The values of q_m at 30, 40, and 50ºC were used to perform the calculation, yielding values of 38.42-39.08 m^2/g.

4.5. Adsorption thermodynamics

The relationship between the free Gibbs energy (ΔG^0), enthalpy (ΔH^0), and entropy (ΔS^0) is given by the equation of Gibbs-Helmholtz (Eq. (7)) [24]:

$$\Delta G^0 = \Delta H^0 - T\Delta S^0 \quad (7)$$

At the same time, the relationship between the Gibbs free energy and the equilibrium constant is given by the van't Hoff equation (Eq. (8)) [24]:

$$\Delta G^0 = -RT\ln K_L \quad (8)$$

When the van't Hoff equation is substituted in Gibbs-Helmholtz equation, this lead to Eq. (9):

$$\ln K_L = \frac{\Delta S^0}{R} - \frac{\Delta H^0}{RT} \quad (9)$$

Table 4 shows the values of free Gibbs energy, entropy, and enthalpy. The free Gibbs energy values indicate that the adsorption process is non-spontaneous, but they are low and close to zero, indicating a feasible process that can reach thermodynamic equilibrium at low temperatures for both dyes. Also, MB and CR exhibit an exothermic process; however, the low enthalpy values (0 to -20 kJ/mol) for MB adsorption indicate physisorption [27]. While

CR shows an enthalpy range of -80 to -400 kJ/mol, this is likely due to chemisorption [27]. The negative entropy value indicates that when the colorant molecules are adsorbed onto the guava seed surface, they attain a more ordered state.

The physisorption of MB and guava seed is performed mainly by electrostatic interactions between the positive charges of MB and the negative charges of guava seed (OH^-, $COOH^-$). While chemisorption between CR and guava seeds is probably mediated by the amino and azo groups of CR by chemical coordination with the hydrogen from the hydroxyl groups of the guava seeds.

Table 4. Gibbs free energy, enthalpy, and entropy thermodynamic parameters for MB and CR were estimated at 30, 40, and 50 ºC as the adsorption temperature.

Dyes	**MB**			**CR**		
Temperature, ºC	**ΔG^O, J/mol**	**ΔH^O, J/mol**	**ΔS^O, J/mol.K**	**ΔG^O, J/mol**	**ΔH^O, J/mol**	**ΔS^O, J/mol.K**
30	2837.8			2666.6		
40	3187.6	-17132.7		4999.6	-68017.67	-233.17
50	4162.2		-65.6	7331.3		

5.0. Conclusions and Future Recommendations

The guava seed is a promising adsorbent for MB and CR dyes. An 80ºC temperature was selected to maintain the availability of most functional groups for adsorption. It was found that both colorant adsorption processes were exothermic; increasing temperature positively affected the maximum adsorption capacity. However, the low enthalpy of MB indicates that physisorption is mainly driven by electrostatic interactions between the negatively charged groups of the guava seed (OH-, COOH-) and the positively charged groups of MB. While CR adsorption is a chemisorption, probably carried out by the amino and azo groups of CR, and the chemical coordination with hydrogen binding of hydroxyl groups from guava seed. Future work recommendations are:

- Increase the specific surface area of ground guava seed, reducing the particle diameter by grinding.
- Increase the specific surface area of ground guava seed when phosphoric acid is impregnated at low concentration to generate a mesoporous structure.
- Chemical modification of the surface area with citric acid to add additional carboxylic acids (-COOH).
- Chemical modification by oxidation with hydrogen peroxide or nitric acid to increase hydroxyl (-OH), and carboxylic acids (-COOH).
- Estimate the average pore diameter and specific surface area using N_2 physisorption experiments.
- Analyze the amount of hydroxyl and carboxylic groups by the Boehm titration method.
- Repeat the adsorption experiments with methylene blue and Congo red with the aim of increasing the maximum adsorption capacity.

Declarations

Source of Funding

This study did not receive any grant from funding agencies in the public or not-for-profit sectors.

Conflict of Interest

The authors declare no conflicts of interest.

Consent for Publication

The authors declare that they consented to the publication of this study.

Authors' contribution

DACM and JACR conceived and designed the study. JAMP, SAHJ, and LKUD performed experiments and collected the data. LFCS and TEFG analyzed the data. DACM wrote the first draft of the manuscript. All authors read, revised, and approved the final manuscript.

Informed Consent

Not applicable.

Availability of data and material

All data is included within the article.

Institutional Review Board Statement

Not applicable.

Ethical Approval

Not applicable.

Acknowledgement

LKUD acknowledges the fellowship support provided by the Secretaría de Ciencia, Humanidades, Tecnología e Innovación (SECIHTI) (fellowship/CVU number: 1274469).

Declaration of Artificial Intelligence

Not applicable.

References

[1] Bentahar, S., Dbik, A., El Khomri, M., El Messaoudi, N., & Lacherai, A. (2017). Adsorption of methylene blue, crystal violet and congo red from binary and ternary systems with natural clay: Kinetic, isotherm, and thermodynamic studies. Journal of Environmental Chemical Engineering, 5: 5921–5932. https://doi.org/10.1016/j.jece.2017.11.003.

[2] Lellis, B., Fávaro-Polonio, C.Z., Pamphile, J.A., & Polonio, J.C. (2019). Effects of textile dyes on health and the environment and bioremediation potential of living organisms. Biotechnology Research and Innovation, 3: 275–290. https://doi.org/10.1016/j.biori.2019.09.001.

[3] Katheresan, V., Kansedo, J., & Lau, S.Y. (2018). Efficiency of various recent wastewater dye removal methods: A review. Journal of Environmental Chemical Engineering, 6: 4676–4697. https://doi.org/10.1016/j.jece.2018.06.060.

[4] Deng, D., Lamssali, M., Aryal, N., Ofori-Boadu, A., Jha, M.K., & Samuel, R.E. (2020). Textiles wastewater treatment technology: A review. Water Environment Research, 92: 1805–1810. https://doi.org/10.1002/wer.1437.

[5] Islam, M.T., Al Mamun, M.A., Halim, A.F.M.F., Peila, R., & Sanchez Ramirez, D.O. (2024). Current trends in textile wastewater treatment—Bibliometric review. Environmental Science and Pollution Research, 31: 19166–19184. https://doi.org/10.1007/s11356-024-32454-3.

[6] Shi, Y., Chang, Q., Zhang, T., Song, G., Sun, Y., & Ding, G. (2022). A review on selective dye adsorption by different mechanisms. Journal of Environmental Chemical Engineering, 10(6): 108639. https://doi.org/10.1016/j.jece.2022.108639.

[7] Lu, J., Zhou, Y., & Zhou, Y. (2023). Recent advance in enhanced adsorption of ionic dyes from aqueous solution: A review. Critical Reviews in Environmental Science and Technology, 53(19): 1709–1730. https://doi.org/10.1080/10643389.2023.2200714.

[8] Dutta, S., Gupta, B., Srivastava, S.K., & Gupta, A.K. (2021). Recent advances on the removal of dyes from wastewater using various adsorbents: A critical review. Materials Advances, 2(14): 4497–4531. https://doi.org/10.1039/d1ma00354b.

[9] Haleem, A., Shafiq, A., Chen, S.-Q., & Nazar, M. (2023). A comprehensive review on adsorption, photocatalytic and chemical degradation of dyes and nitro-compounds over different kinds of porous and composite materials. Molecules, 28(3): 1081. https://doi.org/10.3390/molecules28031081.

[10] Farhadi, A., Ameri, A., & Tamjidi, S. (2021). Application of agricultural wastes as a low-cost adsorbent for removal of heavy metals and dyes from wastewater: A review study. Physical Chemistry Research, 9(2): 211–226. https://doi.org/10.22036/pcr.2021.256683.1852.

[11] Kadhom, M., Albayati, N., Alalwan, H., & Al-Furaiji, M. (2020). Removal of dyes by agricultural waste. Sustainable Chemistry and Pharmacy, 16: 100259. https://doi.org/10.1016/j.scp.2020.100259.

[12] Mansour, R., Simeda, M.G., & Zaatout, A. (2020). Adsorption studies on brilliant green dye in aqueous solutions using activated carbon derived from guava seeds by chemical activation with phosphoric acid. Desalination and Water Treatment, 202: 396–409. https://doi.org/10.5004/dwt.2020.26147.

[13] Hashem, A., Aniagor, C.O., Farag, S., & Aly, A.A. (2025). Adsorption of acid violet 90 dye onto activated carbon and guava seed powder adsorbents. Biomass Conversion and Biorefinery, 15: 25825–25839. https://doi.org/10.1007/s13399-023-04758-w.

[14] Ponnuchamy, M., Kapoor, A., Pakkirisamy, B., Sivaraman, P., & Ramasamy, K. (2020). Optimization, equilibrium, kinetic and thermodynamic studies on adsorptive remediation of phenol onto natural guava leaf

powder. Environmental Science and Pollution Research, 27(17): 20576–20597. https://doi.org/10.1007/s11356-019-07145-z.

[15] Hashem, A., Amr, A., Abdel-Halim, E.S., Farag, S., & Aly, A.A. (2025). Eco-friendly chromium(VI) cleanup: Guava seed biosorbent performance in equilibrium, kinetic, and thermodynamic studies. Current Research in Green and Sustainable Chemistry, 11: 100492. https://doi.org/10.1016/j.crgsc.2025.100492.

[16] Tapia-Quiroz, G.E., Valencia-Leal, S.A., Vázquez-Guerrero, A., Alfaro-Cuevas-Villanueva, R., Escudero-García, R., & Cortés-Martínez, R. (2025). Surfactant-enhanced guava seed biosorbent for lead and cadmium removal: Kinetics, thermodynamics, and reusability insights. Sustainable Chemistry, 6(1): 5. https://doi.org/10.3390/suschem6010005.

[17] Marzuki, M., Jawad, A.H., Zazulir, N.I.I.M., Deris, R.R.R., Wu, R., & AlOthman, Z.A. (2025). High surface area activated carbon with mesoporous structure from pyrolyzed *Psidium guajava* L. peel: Characterization and experimental design optimization for methyl violet 2B dye removal. Diamond and Related Materials, 159(Part B): 112869. https://doi.org/10.1016/j.diamond.2025.112869.

[18] Ojedokun, A.T., & Bello, O.S. (2017). Kinetic modeling of liquid-phase adsorption of Congo red dye using guava leaf-based activated carbon. Applied Water Science, 7(4): 1965–1977. https://doi.org/10.1007/s13201-015-0375-y.

[19] Abdullah, M.F., & Othman, N.F. (2023). Physicochemical and adsorption properties of guava leaves-activated carbon by hydrochloric acid on adsorption of methylene blue. Scientific Research Journal, 20(1): 33–49. https://doi.org/10.24191/srj.v20i1.20669.

[20] Abdulla, N.K., Alzahrani, E.A., Dwivedi, P., Goel, S., Hafeez, S., Khulbe, M., Siddiqui, S.I., & Oh, S. (2024). MnO_2 decoration onto the guava leaves: A sustainable and cost-effective material for methylene blue dye removal. Heliyon, 10(14): e34267. https://doi.org/10.1016/j.heliyon.2024.e34267.

[21] de Almeida, E., Pacheco, E., Nagahama, K., Santos, T.S., & de Souza, A. (2024). Adsorption kinetics of tartrazine dye on activated carbon derived from guava (*Psidium guajava*) seeds. Journal of the Brazilian Chemical Society, 35(12): e-20240139. https://doi.org/10.21577/0103-5053.20240139.

[22] Abdulla, N.K., Alzahrani, E.A., Munshi, G.H., AL-Balawi, A.M., Al-Malwi, S.D., Alsebaii, N.M., Hafeez, S., Oh, S., & Chaudhry, S.A. (2026). Manganese ferrite/guava leaf nano-bio composite for adsorptive removal of methylene blue dye from water. Molecules, 31(10): 1754. https://doi.org/10.3390/molecules31101754.

[23] Elizalde-González, M.P., & Hernández-Montoya, V. (2009). Guava seed as an adsorbent and as a precursor of carbon for the adsorption of acid dyes. Bioresource Technology, 100: 2111–2117. https://doi.org/10.1016/j.biortech.2008.10.056.

[24] Gao, J.J., Qin, Y.B., Zhou, T., Cao, D.D., Xu, P., Hochstetter, D., & Wang, Y.F. (2013). Adsorption of methylene blue onto activated carbon produced from tea (*Camellia sinensis* L.) seed shells: Kinetics, equilibrium,

and thermodynamics studies. Journal of Zhejiang University Science B, 14(7): 650–658. https://doi.org/10.1631/jzus.b12a0225.

[25] Musah, M., Azeh, Y., & Mathew, J.T. (2022). Adsorption kinetics and isotherm models: A review. Caliphate Journal of Science and Technology, 4(1): 21–27. https://doi.org/10.4314/cajost.v4i1.3.

[26] Hang, P.T., & Brindley, G.W. (1970). Methylene blue adsorption by clay minerals: Determination of surface areas and cation exchange capacities (clay-organic studies XVIII). Clays and Clay Minerals, 18(4): 203–212. https://doi.org/10.1346/ccmn.1970.0180404.

[27] Húmpola, P.D., Odetti, H.S., Fertitta, A.E., & Vicente, J.L. (2013). Thermodynamic analysis of adsorption models of phenol in liquid phase on different activated carbons. Journal of the Chilean Chemical Society, 58(1): 1541–1544. https://doi.org/10.4067/s0717-97072013000100009.